crystallization papers

Crystallization and preliminary X-ray diffraction analysis of the 16-haem cytochrome of *Desulfovibrio gigas*

Teresa Santos-Silva,[a] João M. Dias,[a] Gleb Bourenkov,[b] Hans Bartunik,[b] Isabel Moura[a] and Maria João Romão[a]*

[a]REQUIMTE/CQFB Departamento de Química, Faculdade de Ciências e Tecnologia, Universidade Nova de Lisboa, 2829-516 Caparica, Portugal, and [b]Max-Planck Research Unit for Structural Molecular Biology, MPG-ASMB c/o DESY, Notkestrasse 85, 22607 Hamburg, Germany

Correspondence e-mail: mromao@dq.fct.unl.pt

High-molecular-weight cytochromes (Hmcs) belong to a large family of multihaem cytochromes in sulfate-reducing bacteria. HmcA is the first cytochrome reported to have 16 *c*-type haems arranged in its polypeptide chain. The function of this cytochrome is still unknown, although it is clear that it belongs to a membrane-bound complex involved in electron transfer from the periplasm to the membrane. HmcA from *Desulfovibrio gigas* has been purified and successfully crystallized using the hanging-drop vapour-diffusion method. The crystals grew using PEG and zinc acetate as precipitants to maximum dimensions of $0.2 \times 0.2 \times 0.2$ mm in an orthorhombic space group, with unit-cell parameters $a = 88.9$, $b = 90.9$, $c = 83.7$ Å. The crystals diffracted to beyond 2.07 Å and a MAD data set was collected.

1. Introduction

HmcA is a high-molecular-weight cytochrome with 16 *c*-type haems arranged in a polypeptide chain of ~550 amino acids. It has been found in the periplasm of some species of sulfate-reducing bacteria of the *Desulfovibrio* genus: *D. vulgaris* Hildenborough (Higuchi *et al.*, 1987), *D. vulgaris* Miyazaki (Ogata *et al.*, 1993) and *D. gigas* (Chen *et al.*, 1994).

This cytochrome is part of a membrane-bound complex that is encoded by the *hmc* operon (Rossi *et al.*, 1993) and has high resemblance to the 9Hc complex present in *D. desulfuricans* species (Saraiva *et al.*, 1999). Both complexes contain a multihaem cytochrome, membrane-bound and integral membrane proteins, which contain haems and/or Fe–S clusters. Their function is not yet fully understood, but it is known that they transfer electrons from the periplasm to the membrane, either to the membranous quinone pool (Simon, 2002) or for cytoplasmic sulfate reduction (Rossi *et al.*, 1993).

The structure of *D. vulgaris* Hildenborough HmcA has recently been published (Czjzek *et al.*, 2002; Matias *et al.*, 2002). It can be sub-divided into three different domains related to the structure of well known cytochromes from *Desulfovibrio* bacteria. The N-terminal region is homologous to the three-haem-containing cytochrome c_7, the second domain to the four-haem cytochrome c_3 and the last domain is related to the nine-haem cytochrome 9HcA. Cytochrome c_3 is thought to be the electronic shuttle between Fe-hydrogenase and HmcA, as found in the case of the nine-haem cytochrome. A structural model of HmcA with cytochrome c_3 from *D. vulgaris* Hildenborough was proposed, showing the possible sites for this haem–haem interaction (Czjzek *et al.*, 2002).

Another feature of this low-redox-potential cytochrome is that it only has 15 haem-binding sites of the c_3 type (Cys-*X*-*X*-Cys-His). The remaining haem is a high-spin haem with only five ligands in its coordination sphere; hydrophobic residues surround the Fe atom, protecting it against solvent interactions. This could be an active site for an unknown enzymatic role of the protein, resembling that observed in other *c*-type haem-containing proteins such as cytochrome *c* nitrite reductase (Cunha *et al.*, 2003).

In this work, we aim to determine the three-dimensional structure of HmcA from *D. gigas* and compare it with the homologous *D. vulgaris* structure (sequence identity of 39.6%), the only Hmc structure available so far (Czjzek *et al.*, 2002; Matias *et al.*, 2002), which may help in the understanding of the physiological role of HmcA.

2. Materials and methods

2.1. Purification

D. gigas NCIB 9332 cells were obtained from 300 l growth in lactate–sulfate medium at 277 K under anaerobic conditions (LeGall *et al.*, 1965).

The purification, which was performed at 277 K, began by disrupting and centrifuging the cells in two stages: firstly at 9500 rev min^{-1} for 65 min and subsequently at 42 000 rev min^{-1} for 75 min in order to eliminate the cell membranes. The soluble extract was then dialysed against 5 m*M* Tris–HCl buffer pH 7.6 overnight and loaded onto a DEAE-52 column (52×4.5 cm). A linear

gradient of Tris–HCl buffer (10–250 mM, pH 7.6) was applied and the fraction at 150 mM ionic strength which contained cytochromes was collected. After dialysis and concentration, this fraction was loaded onto a Resource-Q 6 ml column (Pharmacia) and eluted with a Tris–HCl buffer gradient (10–250 mM, pH 7.6). The fraction containing cytochromes, which eluted at 80 mM ionic strength, was concentrated to approximately 10 mg ml^{-1} and crystallization assays were performed.

Purification was checked by UV–visible spectra (UV-160A, Shimadzu) and SDS–PAGE (Bio-Rad), according to the description in Chen *et al.* (1994).
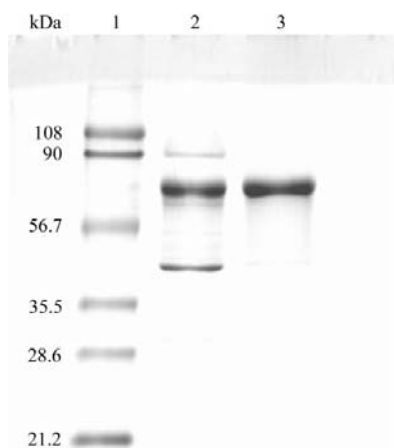

Figure 1
12.5% SDS–PAGE of HmcA purification. Lane 1, Bio-Rad low-range prestained standards. Lane 2, protein fraction used for crystallization. Lane 3, dissolved HmcA crystals.
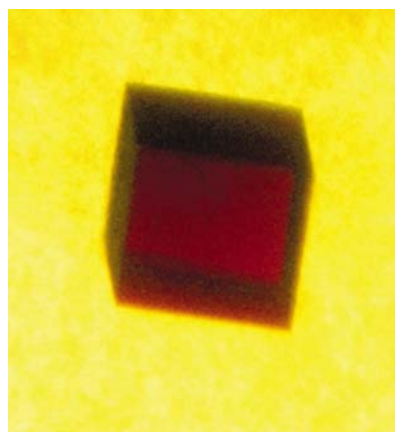
The protein used for crystallization contained extra bands in SDS–PAGE in addition to the HmcA band at 67 kDa. However, the gel obtained from dissolved crystals proved its final purity (Fig. 1).

2.2. Crystallization

Crystallization assays were carried out using the hanging-drop vapour-diffusion method at 293 K. Initial crystallization conditions were screened using an in-house modified version of the sparse-matrix method of Jancarik & Kim (1991), in combination with the commercial Hampton Research (California, USA) Crystal Screen and Crystal Screen 2.

Plate-shaped crystals grew within one week in drops consisting of 2 µl protein solution and 4 µl reservoir solution (12% PEG 8K, 50 mM zinc acetate pH 6.5), but were of insufficient quality for diffraction experiments. The macroseeding technique proved to be the best approach to further improve the crystals, which reached maximum dimensions of approximately 0.2 × 0.2 × 0.2 mm with a cubic shape (Fig. 2). The HmcA crystals were harvested from the mother liquor and soaked for a few seconds in a cryoprotectant solution containing 30% glycerol.

In order to determine the three-dimensional structure of HmcA, a multiple-wavelength anomalous diffraction (MAD) experiment was performed at the iron edge and data collection was performed at the BW6 beamline of the MPG-ASMB in DESY (Hamburg, Germany) using a CCD detector and synchrotron radiation at ~100 K.

3. Results and discussion

Initially, a fluorescence scan was performed on a crystal in order to determine the exact wavelengths for the data collection. Two wavelengths were selected near the K absorption edge of the Fe atom (1.738 and 1.744 Å) and a third wavelength at a high-energy remote point (1.050 Å). At this wavelength the crystals diffracted to beyond 2.07 Å resolution (Fig. 3).

X-ray data were processed with *DENZO* and *SCALEPACK* (Otwinowski & Minor, 1997) in space group $P2_12_12$, with unit-cell

Table 1
Data-collection statistics of X-ray diffraction data.

Values in parentheses are for the highest resolution shell.

Wavelength (Å)	1.738	1.744	1.050
No. observed reflections	143942	144937	215777
No. unique reflections	50643	50752	74840
Redundancy	2.8 (2.8)	2.8 (2.8)	2.9 (2.6)
Resolution limits (Å)	25–2.40 (2.49–2.40)	25–2.40 (2.49–2.40)	20–2.10 (2.17–2.10)
R_{merge} (%)	3.7 (24.0)	3.1 (25.0)	3.9 (39.6)
Completeness (%)	98.9 (98.6)	98.9 (98.8)	97.5 (96.1)
Average $I/\sigma(I)$	24.2 (4.40)	29.0 (4.27)	22.5 (2.84)
Mosaicity (°)	1.0	1.0	1.0

Figure 2
A crystal of HmcA from *D. gigas* grown with 12% PEG 8K, 50 mM zinc acetate pH 6.5. Regular cubic shaped crystals with dimensions of ~0.2 × 0.2 × 0.2 mm were obtained by the hanging-drop vapour-diffusion method followed by macroseeding techniques.
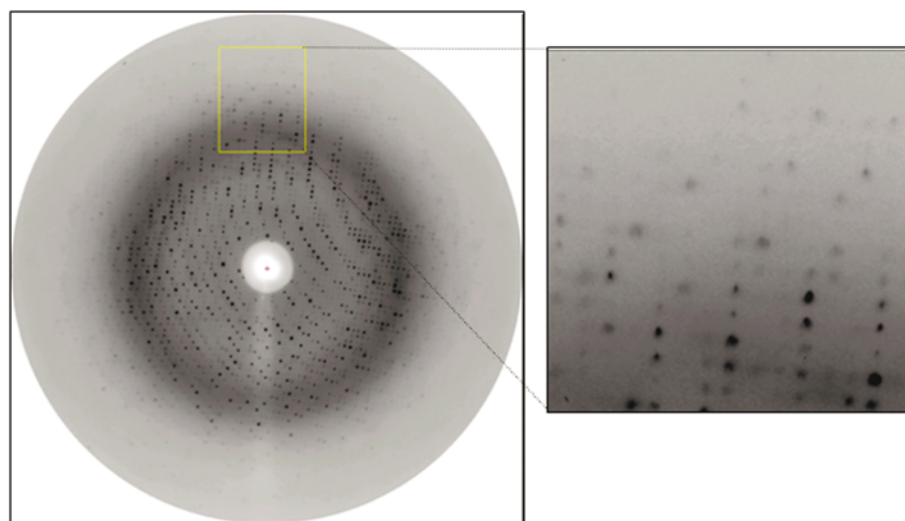

Figure 3
0.4° oscillation image of a cryocooled HmcA crystal taken using a CCD detector on BW6 beamline of the MPG-ASMB at DESY. A close-up is shown on the right. The frame edge is at 2.0 Å resolution. Image displayed using *MOSFLM* (Leslie, 1992).
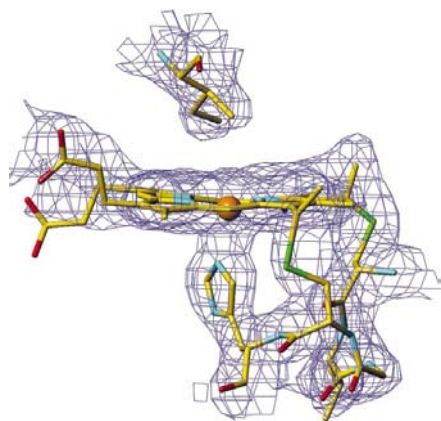
Figure 4
Experimental $2F_o - F_c$ electron-density map around haem 15 after density modification, contoured at the 1σ level, superimposed with the corresponding model. Haem 15 is the high-spin haem, with only one axial ligand in its coordination sphere. The figure was created using *TURBO-FRODO* (Roussel & Cambillau (1991).

parameters $a = 88.9$, $b = 90.9$, $c = 83.7$ Å. Details of data collection and statistics are summarized in Table 1. The Matthews coefficient is 2.6 Å^3 Da^{-1}, assuming the presence of one molecule in the asymmetric unit, corresponding to a solvent content of 53% (Matthews, 1968).

The strong anomalous signal produced by the 16 Fe atoms in the protein allowed us to obtain initial phases and, using *SOLVE* (Terwilliger & Berendzen, 1999) in the resolution range 20.0–2.4 Å, the 16 expected sites were found. The initial mean figure of merit of 0.53 was further improved to 0.85 by density-modification procedures assuming a solvent content of 38% and using *SOLOMON* through the *SHARP* interface (de La Fortelle & Bricogne, 1997).

The good quality of the experimental maps enabled identification of the porphyrin rings of all haems plus their axial ligands. The electron density at the high-spin haem is represented in Fig. 4. Manual model building and refinement are now in progress.

References

Chen, L., Pereira, M. M., Teixeira, M., Xavier, A. V. & LeGall, J. (1994). *FEBS Lett.* **347**, 295–299.

Cunha, C. A., Macieira, S., Dias, J. M., Almeida, G., Goncalves, L. L., Costa, C., Lampreia, J., Huber, R., Moura, J. J., Moura, I. & Romao, M. J. (2003). *J. Biol. Chem.* **278**, 17455–17465.

Czjzek, M., El Antak, L., Zamboni, V., Morelli, X., Dolla, A., Guerlesquin, F. & Bruschi, M. (2002). *Structure*, **10**, 1677–1686.

Higuchi, Y., Inaka, K., Yasuoka, N. & Yagi, T. (1987). *Biochim. Biophys. Acta*, **911**, 341–348.

Jancarik, J. & Kim, S.-H. (1991). *J. Appl. Cryst.* **24**, 409–411.

La Fortelle, E. de & Bricogne, G. (1997). *Methods Enzymol.* **276**, 472–494.

LeGall, J., Mazza, G. & Dragoni, N. (1965). *Biochim. Biophys. Acta*, **99**, 385–387.

Leslie, A. G. W. (1992). *Jnt CCP4/ESF–EAMCB Newsl. Protein Crystallogr.* **26**, 27–33.

Matias, P. M., Coelho, A. V., Valente, F. M. A., Plácido, D., LeGall, J., Xavier, A. V., Pereira, I. A. C. & Carrondo, M. A. (2002). *J. Biol. Chem.* **277**, 47907–47916.

Matthews, B. W. (1968). *J. Mol. Biol.* **33**, 491–497.

Ogata, M., Kiuchi, N. & Yagi, T. (1993). *Biochimie*, **75**, 977–983.

Otwinowski, Z. & Minor, W. (1997). *Methods Enzymol.* **276**, 307–326.

Rossi, M., Pollock, W. B., Reij, M. W., Keon, R. G., Fu, R. & Voordouw, G. (1993). *J. Bacteriol.* **175**, 4699–4711.

Roussel, A. & Cambillau, C. (1991). *TURBO-FRODO: A Tool for Building Structural Models.* Mountain View, CA, USA: Silicon Graphics.

Saraiva, L. M., Costa, P. N. & LeGall, J. (1999). *Biochem. Biophys. Res. Commun.* **262**, 629–634.

Simon, J. (2002). *FEMS Microbiol. Rev.* **26**, 285–309.

Terwilliger, T. C. & Berendzen, J. (1999). *Acta Cryst.* D**55**, 849–861.